Electronic Supplementary Material (ESI) for Journal of Materials Chemistry A.
This journal is © The Royal Society of Chemistry 2019

**Plasma-Engineered 1T/2H Phases in 3D-Hierarchical $WSe_2$ Nanoscrews as High Performance NO Gas Sensors with ppb-level Detection Limit**

Yu-Ze Chen[a, b, d], Shao-Hsin Lee[a, b], Teng-Yu Su[a, b], Shu-Chi Wu[a, b], Pin-Jung Chen[a, b] and Yu-Lun Chueh*[, a, b, c]

[a]Department of Materials Science and Engineering, National Tsing Hua University, Hsinchu 30013, Taiwan, ROC

[b]Frontier Research Center on Fundamental and Applied Sciences of Matters, National Tsing Hua University, Hsinchu 30013, Taiwan ROC

[c]Department of Physics, National Sun Yat-Sen University, Kaohsiung, 80424, Taiwan.

[d]Department of Materials Science and Engineering, National Cheng Kung University, Tainan 701, Taiwan, ROC

*E-mail: ylchueh@mx.nthu.edu.tw

We estimate relative surface areas of nanostructure by electrochemically active surface area method (ECSA). The electrochemically active surface area (ECSA) of samples was usually estimated using using cyclic voltammetry measurement. (Refs. 2-3) The surface area of the sample was calculated by the double layer capacitance according to the following formula:

ECSA=Cdl / Cs

However, it is quite challenging to obtain the exact surface area of our material due to the unknown capacitive behavior (Cs) of the $WSe_2$, especially in 1D nanostructure. Therefore, we can simply estimate relative surface areas of our two samples, which are flat and nanoscrews since the double layer capacitance (Cdl) is expected to be linearly proportional to effective active surface area where the approach to estimate surface area was also commonly employed in previous reports. (Ref 4) The capacitance can be calculated from the scan rate as a function of the current density, which is twice of Cdl by extracting slopes from ΔJ versus scan rates as shown in Figure 2c. It is observed that the capacitance obtained from the nanostructured sample (Cdl of 14.4 μF cm-2) is approximately two orders of magnitude higher than that of the flat film ($C_{dl}$ of 0.09 μF $cm^{-2}$). We have added this part into the supporting information.

Table S1. The double layer capacitance (Cdl) and the relative surface areas of flat $WSe_2$ and $WSe_2$ nanoscrews.

| **Structure** | **Capacitance (μF/$cm^2$)** | **Surface area related to flat $WSe_2$** |
|---|---|---|
| **Flat** | 0.09 | 1 |
| **Nanoscrews** | 14.4 | 160 |

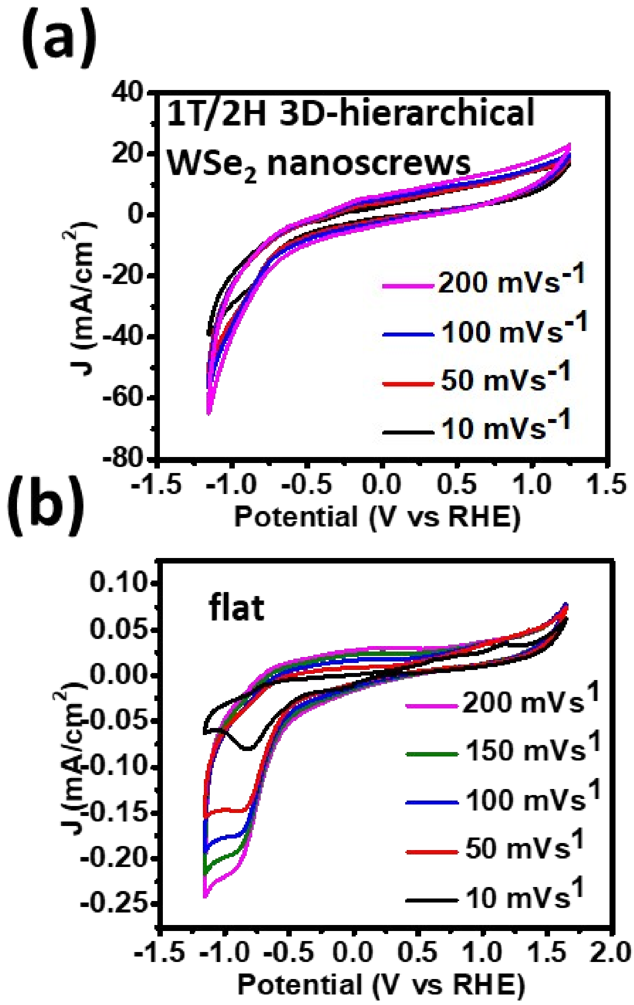


**Figure S1** Results of cyclic voltammetry measurement for (a) $WSe_2$ nanoscrews. (b) flat $WSe_2$.

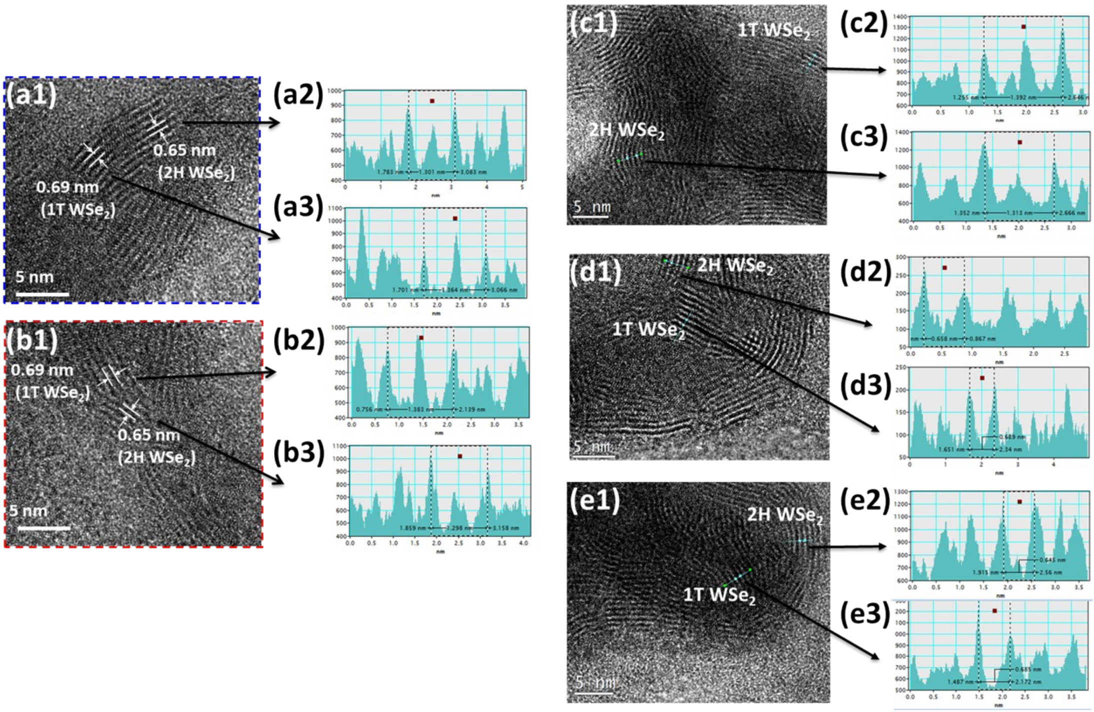


**Figure S2** TEM images of 1T/2H of 1T/2H 3D-hierarchical $WSe_2$ nanoscrews for 5 random area (a1)-(e1) and the corresponded intensity profile for 2H and 1T phase (a2)-(e2), (a3)-(e3), respectively.

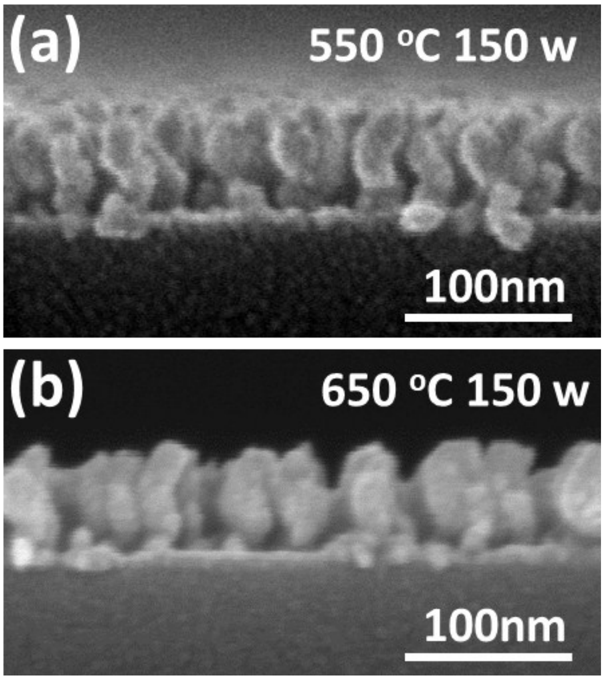


**Figure S3** SEM images of 3D-hierarchical $WSe_2$ nanoscrews synthesized at (a) 550$^{o}$C (b) 650$^{o}$C with plasma 150 W.

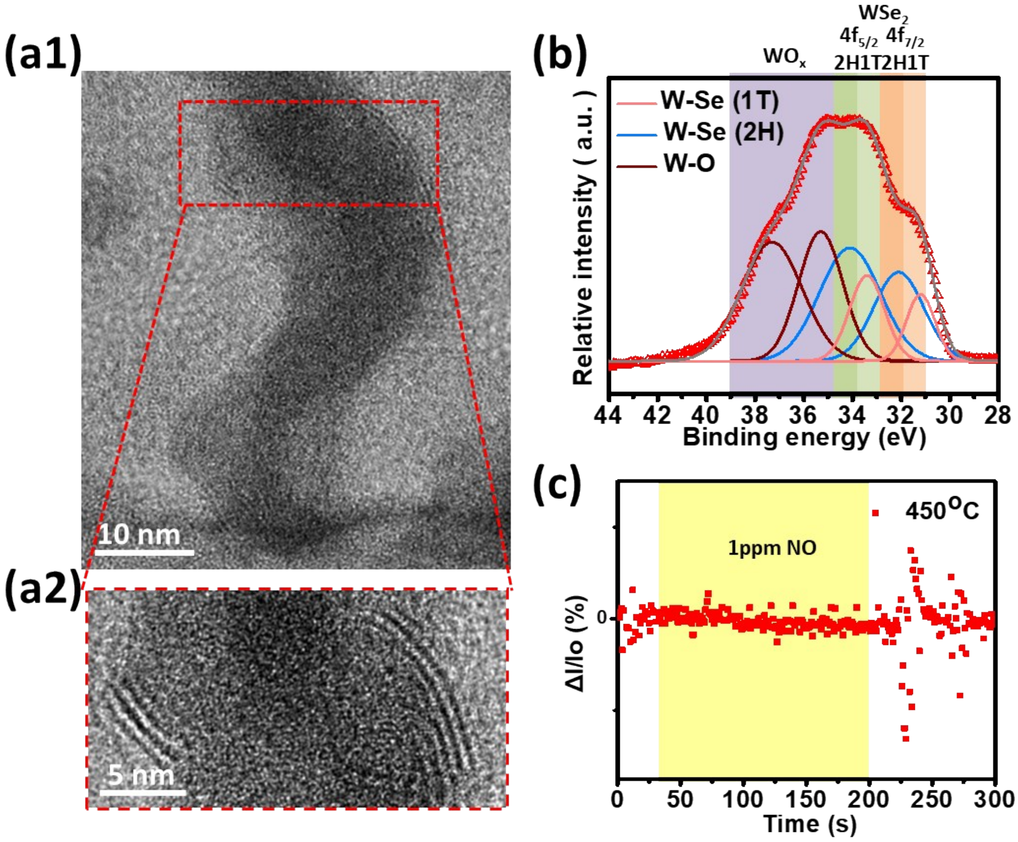


**Figure S4** (a1)-(a2) TEM images of 3D-hierarchical $WSe_2$ nanoscrews selenized without plasma function. (b) XPS results of W 4f (c) Results of gas response upon 1 ppm NO gas.

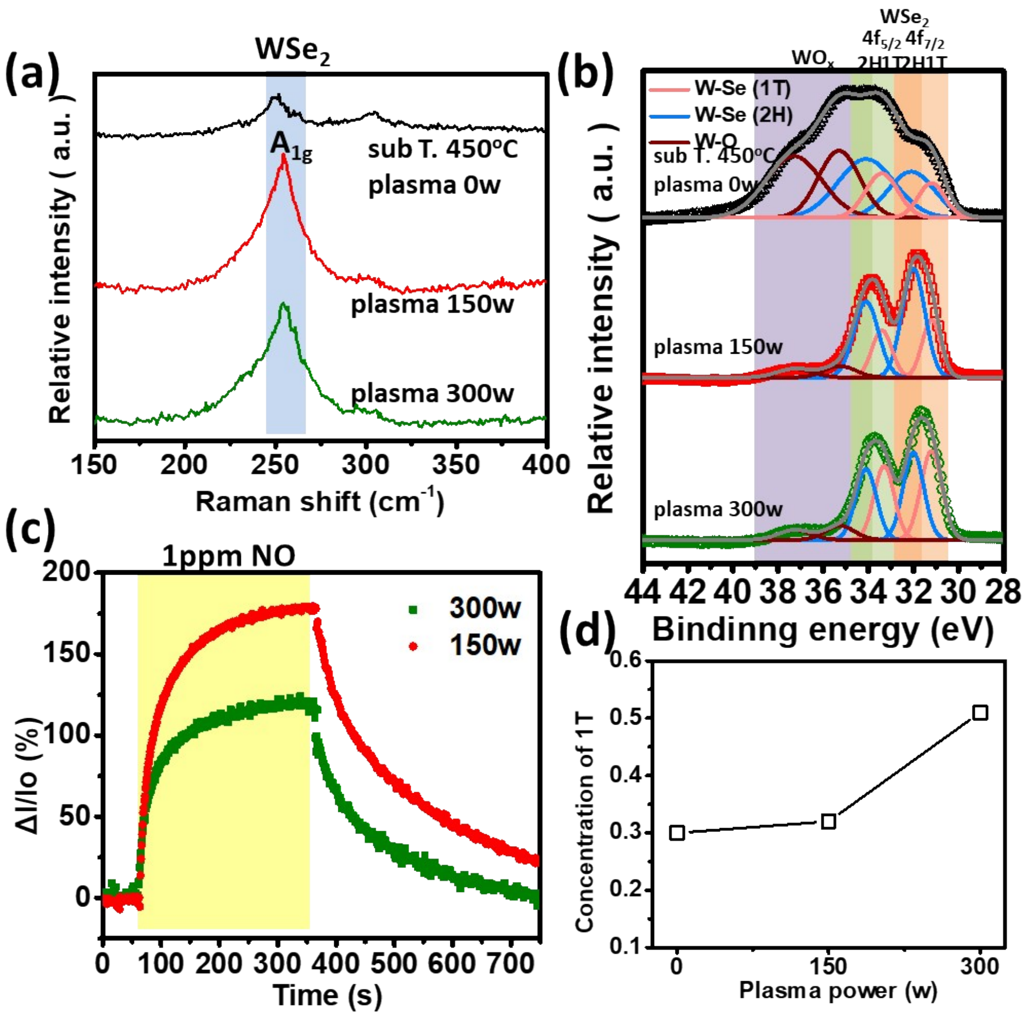


**Figure S5** (a) Raman spectra of 3D-hierarchical $WSe_2$ nanoscrews synthesized at 450 $^{o}$C with 150 and 300 W. (b) XPS spectra of W 4f of $WSe_2$ (c) Results of gas response of 3D-hierarchical $WSe_2$ nanoscrews synthesized at 450 $^{o}$C with 150 and 300 W upon 1 ppm NO gas. (d) Concentration of 1T as dependence of plasma power.

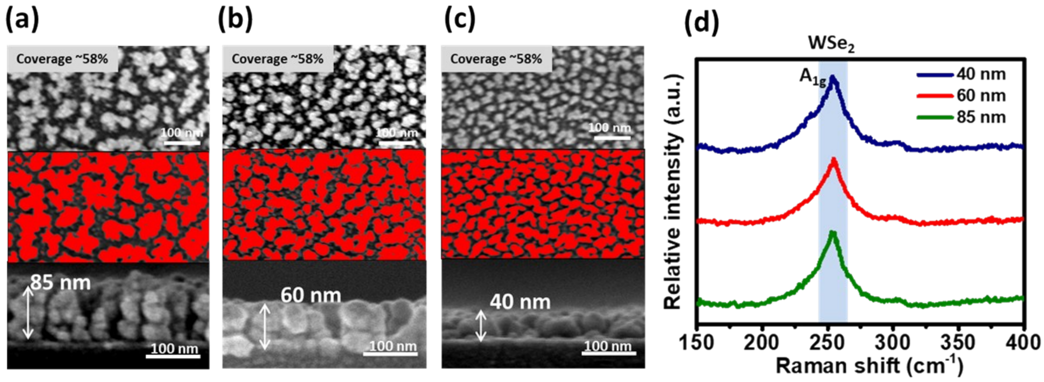


**Figure S6** SEM images of 3D-hierarchical $WSe_2$ nanoscrews with heights of (a) 85 nm (b) 60 nm (c) 40 nm. Note that the coverage was kept as 58 % estimated by software image J. (d) Raman spectra of 3D-hierarchical $WSe_2$ nanoscrews as a dependence of height.

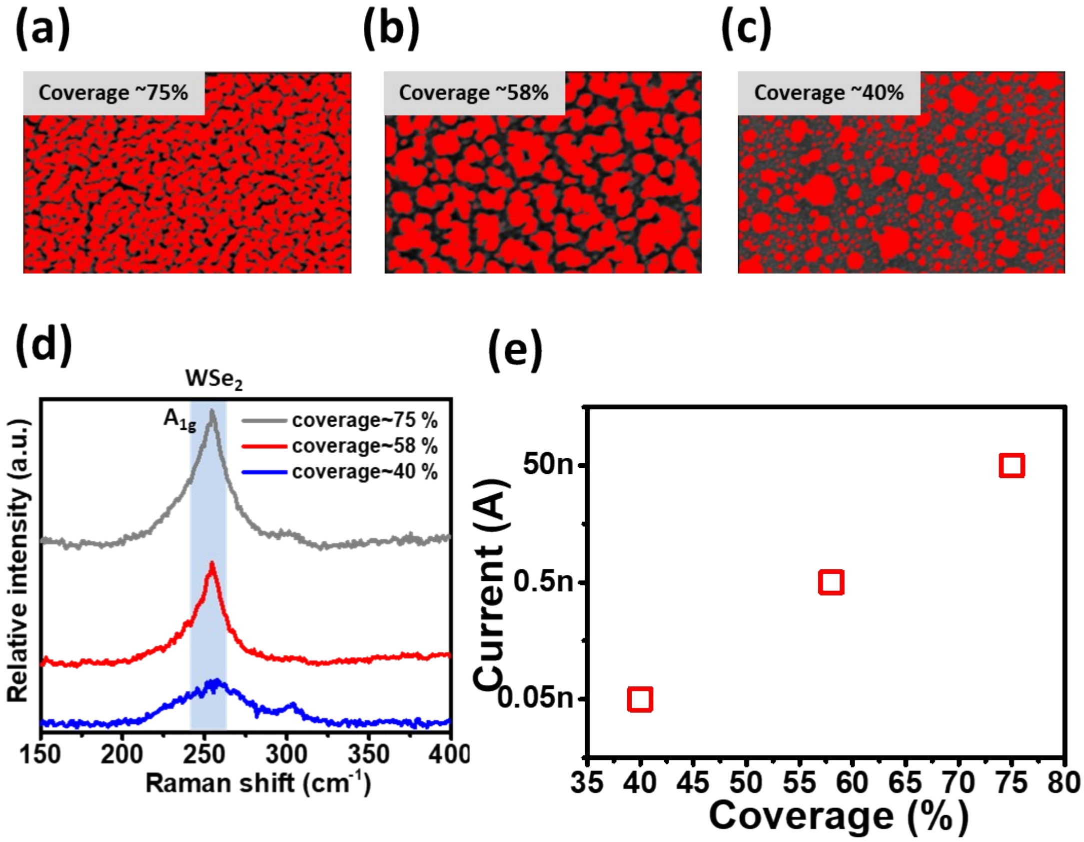


**Figure S7** SEM images of 3D-hierarchical $WSe_2$ nanoscrews with coverages of (a) 75 % (b) 58 % (c) 40 %. Note that the height was kept as 60 nm. (d) Raman spectra of 3D-hierarchical $WSe_2$ nanoscrews as a dependence of coverages. (e) Base current of 3D-hierarchical $WSe_2$ nanoscrews as a dependence of coverages.

**Reference**

(1) S. Brunauer, P. H. Emmett and E. Teller, Adsorption of Gases in Multimolecular Layers J. Am. Chem. Soc., 60, 309-319 (1938).

(2) Yang Y., Lun Z.Y., Xia G.L., Zheng F.C., He M.N. & Chen Q.W. Non-precious alloy encapsulated in nitrogen-doped graphene layers derived from MOFs as an active and durable hydrogen evolution reaction catalyst. Energy Environ. Sci. 8, 3563-3571 (2015).

(3) Lukowski M.A., Daniel A.S., Meng F., Forticaux A., Li L. & Jin S. Enhanced Hydrogen Evolution Catalysis from Chemically Exfoliated Metallic MoS2 Nanosheets. J.Am.Chem.Soc. 135, 10274−10277 (2013).

(4) Merki, D., Vrubel, H., Rovelli, L., Fierro, S. & Hu, X., Fe, Co, and Ni ions promote the catalytic activity of amorphous molybdenum sulfide films for hydrogen evolution Chem. Sci. 3, 2515-2525 (2015).